

Elbow Joint Geometry in Bears (Ursidae, Carnivora): a Tool to Infer Paleobiology and Functional Adaptations of Quaternary Fossils

Carlo Meloro¹  · Alessandro Marques de Oliveira²

Published online: 9 November 2017

© The Author(s) 2017. This article is an open access publication

Abstract Bears are currently represented by eight species among Carnivora. Being all particularly large and generally plantigrade limits to certain extent their functional morphology so that inferences about their past diversification are difficult to achieve. We analyzed variation in bears' elbow joint size and shape to reconstruct paleobiology of Quaternary fossil species. By using 2D geometric morphometrics, we were able to discriminate with high degree of accuracy species, locomotor and habitat adaptations among extant bears. The giant panda and the spectacled bear are well characterized by an enlarged medial epicondyle, while large members of the genus *Ursus* can be distinguished by their relatively longer and wider trochlea. Elbow joint size varies consistently among ecological categories of extant bears and is generally selected by discriminant function models providing a high degree of classification accuracy (> 80%). American genera *Arctotherium* and *Arctodus* are predicted as non-climbing species potentially adapted to open and mixed environments in agreement with their potentially opportunistic feeding behavior. They retain a wide medial epicondyle probably in relation to a high degree of forelimb dexterity. Cave bears are equally predicted as non-climbers adapted to open habitats while the

middle Pleistocene *Ursus deningeri* and fossil *Ursus arctos* are generally classified as scansorial species with a preference towards mixed habitats. Our study is the first to demonstrate that fragmentary distal epiphyses also can be useful for interpreting functional morphology and ecological adaptations within the family Ursidae.

Keywords Geometric morphometrics · Humerus · Locomotion · Habitat adaptation

Introduction

The postcranial skeleton presents functional adaptations that can be used in ecomorphological studies. The relative size and shape of long bones are significant predictors of locomotory ecology in a multitude groups of extant and fossil mammals (Kappelman 1988; Bishop 1999; Elton 2001; Plummer et al. 2008; Samuels and Van Valkenburgh 2008; Bassarova et al. 2009; Milne et al. 2012; Meloro and Louys 2015; Elton et al. 2016). The order Carnivora exhibits great variation in locomotory modes and environments occupied, which is reflected to some degree in the shape and dimensions of their long bones (Van Valkenburgh 1987; Meloro 2011a; Álvarez et al. 2013; Samuels et al. 2013; Meachen et al. 2015; Tarquini et al. 2017).

Previous studies have indicated that the humerus bone in particular is highly informative to predict locomotor adaptations, predatory behavior, and habitat exploited by both extant and fossil carnivorans (Iwaniuk et al. 2000; Andersson 2004; Schutz and Guralnik 2007; Ercoli et al. 2012; Samuels et al. 2013; Meloro et al. 2013; Martín-Serra et al. 2016; Janis and Figueirido 2014; Fabre et al. 2015a; Tarquini et al. 2017). Besides ecological aspects, the influence of allometry and phylogeny on humerus shape has also been quantified by

Electronic supplementary material The online version of this article (<https://doi.org/10.1007/s10914-017-9413-x>) contains supplementary material, which is available to authorized users.

✉ Carlo Meloro
C.Meloro@ljamu.ac.uk

¹ Research Centre in Evolutionary Anthropology and Palaeoecology, School of Natural Sciences and Psychology, Liverpool John Moores University, Byrom Street, Liverpool L3 3AF, UK

² Universidade Federal do ABC – UFABC, Av. dos Estados, 5001, Bairro Bangu, Santo André, SP, Brazil

geometric morphometric approaches (Ercoli et al. 2012; Fabre et al. 2013a, b, 2015b; Martin-Serra et al. 2014; Botton-Divet et al. 2016, 2017). Size and shape of humeral epiphyses discriminate habitat exploited, feeding strategies, locomotor adaptation, and evolutionary history for many groups of Carnivora (Andersson and Werdelin 2003; Walmsley et al. 2012; Meloro et al. 2013; Figueirido et al. 2015). These studies support the elbow joint (distal humerus epiphysis) as more informative than the humeral proximal epiphysis to infer ecological adaptations in carnivorans due to its load bearing function and its involvement in pronation/supination movements. Herein, we quantify size and shape variation of the elbow joint morphology of extant and fossil species of Ursidae to identify ecomorphological correlates of their locomotory behavior and habitat adaptations.

The family Ursidae currently includes a small species diversity with eight taxa belonging to the subfamily Ursinae. Mostly plantigrade with the exception of the giant panda, *Ailuropoda melanoleuca* (which is semi-plantigrade, Chorn and Hoffmann 1978) and all characterized by generally large body size (Gittleman 1985), the extant bears seem to show homogeneous morphological adaptations to a terrestrial lifestyle, although many of them are good swimmers (i.e., the polar bear, *Ursus maritimus* categorized by some as a semi-aquatic species; De Master and Stirling 1981) and can climb trees (Ortolani and Caro 1996; Samuels et al. 2013). The extant group Ursinae evolved from predatory cursorial Hemicyoninae (Ginsburg and Morales 1998; Stefen 2001) in fast adaptive radiation and with recent speciation events (Goldman et al. 1989; Waits et al. 1999). Interestingly, Ursinae were relatively more diverse during the Quaternary and many authors have suggested climate to have influenced their evolution (Krause et al. 2008; Figueirido and Soibelzon 2010).

Previous ecomorphological approaches with both extant and fossil bears have used mainly cranio-mandibular features to predict autoecological aspects such as feeding habits (Sacco and Van Valkenburgh 2004; Sorkin 2006; Figueirido et al. 2009; Figueirido and Soibelzon 2010). For instance, Figueirido and Soibelzon (2010) were able to identify different ecomorphological adaptations in Tremarctinae bears from South America during the Plio-Pleistocene, concluding that many species were omnivores that possibly behaved as carnivores or herbivores according to resource availability. Isotopic analyses also provided additional data on enigmatic taxa such as *Arctotherium* interpreted as a carnivorous scavenger (Prevosti and Martin 2013; Soibelzon et al. 2014). The Old World cave bear *Ursus spelaeus* received particular attention, too. Generally interpreted as herbivorous based on craniodental morphology (Kurtén 1995; Grandal-d'Anglade and López-González 2005) and isotopic analyses (Bocherens et al. 2006), it appears to show omnivorous morphological adaptations typical of the genus *Ursus* (Figueirido

et al. 2009; Meloro 2011b). Van Heteren et al. (2014, 2016) suggested that cave bear included more foliage in its diet as compared to extant brown bears (*Ursus arctos*). With no doubt, some extinct Ursinae bears were as flexible as extant species in feeding and locomotory behavior (Richards et al. 2008). However, there are few works that have taken into account morphometric approaches on limb bones in bears. Sorkin (2006) reported that short-faced bears *Agriotherium* and *Arctodus* were more herbivorous due to, besides other cranio-mandibular features, absence of adaptations to predatory habits on forelimb bones. Similarly, Figueirido et al. (2010), based on limb dimensions, showed that *Arctodus simus* was not a fast-running super-predator or a specialized scavenger. Given that feeding habits can be correlated with modes of locomotion and habitats exploited, a study on humerus shape might help to elucidate these evolutionary patterns and their connection to environmental changes during the Quaternary.

The aim of the present study is to infer morpho-functional adaptations based on shape and size of the elbow joint in a subsample of extant and Pleistocene bears. The elbow joint reflects function in several groups of mammals such as carnivorans, primates, and rodents (Elton 2001, 2006; Samuels and Van Valkenburgh 2008; Walmsley et al. 2012; Meloro et al. 2013; Elton et al. 2016). Additionally, distal epiphyses are the long bone segments most likely preserved in the fossil record (Elton 2006; Meloro et al. 2013).

Materials and Methods

Institutional Abbreviations

MNHN: Muséum National D'Histoire Naturelle (Paris, France); NHM: Natural History Museum (London, United Kingdom); UFMS: Universidade Federal de Mato Grosso do Sul (Campo Grande, Brazil); WML: World Museum Liverpool (Liverpool, United Kingdom).

Size and Shape Data

Seventy-four humeral epiphyses of extant and fossil specimens belonging to eleven species (Table 1; Table S1) were included in a two dimensional geometric morphometric analysis.

Digital pictures were taken at a fixed distance of one meter on both cranial and caudal views of the elbow joint using a Nikon 3300 digital camera. Specimens were positioned on the ground to ensure parallelism with the camera's optical plane. Thirteen and ten landmarks were defined on cranial and caudal views, respectively, and digitized using the TpsDig 2.17 (Rohlf 2015). The landmarks are of type II, which includes end of the processes and valleys of invaginations (Fig. 1).

Table 1 Sample size of humeri inclusive of extant and fossil (represented by the symbol †) bear taxa

Species	Locomotion	Habitat	Total N	N Males	N Females
<i>Ailuropoda melanoleuca</i>	Semiarboreal	Closed	5	1	
<i>Helarctos malayanus</i>	Semiarboreal	Closed	4		
<i>Melursus ursinus</i>	Semiarboreal	Closed	5	1	1
<i>Tremarctos ornatus</i>	Semiarboreal	Mixed	5	3	1
<i>Ursus americanus</i>	Semiarboreal	Mixed	5	1	1
<i>Ursus arctos</i>	Scansorial	Mixed	12	3	3
<i>Ursus arctos</i> × <i>maritimus</i>	Scansorial	Mixed	1		
<i>Ursus maritimus</i>	No climbing	Open	7	2	3
<i>Ursus thibetanus</i>	Semiarboreal	Closed	9	1	3
<i>Arctodus</i> sp. †			1		
<i>Arctotherium</i> sp. †			1		
<i>Arctotherium bonariense</i> †			1		
<i>Arctotherium wingei</i> †			1		
<i>Ursus arctos</i> †			6		
<i>Ursus deningeri</i> †			1		
<i>Ursus</i> sp. †			3		
<i>Ursus spelaeus</i> †			7		
Tot			74	12	12

For extant species only, locomotion (after Iwaniuk et al. 2000), habitat categorisation (modified after Ortolani and Caro 1996) and number of sexed specimens was included when available

Generalized Procrustes analysis (GPA) was employed to translate, rotate, and scale to the unit centroid size (=CS, the

square root of the sum of squared distances between each landmark to the centroid) the landmark coordinates separately

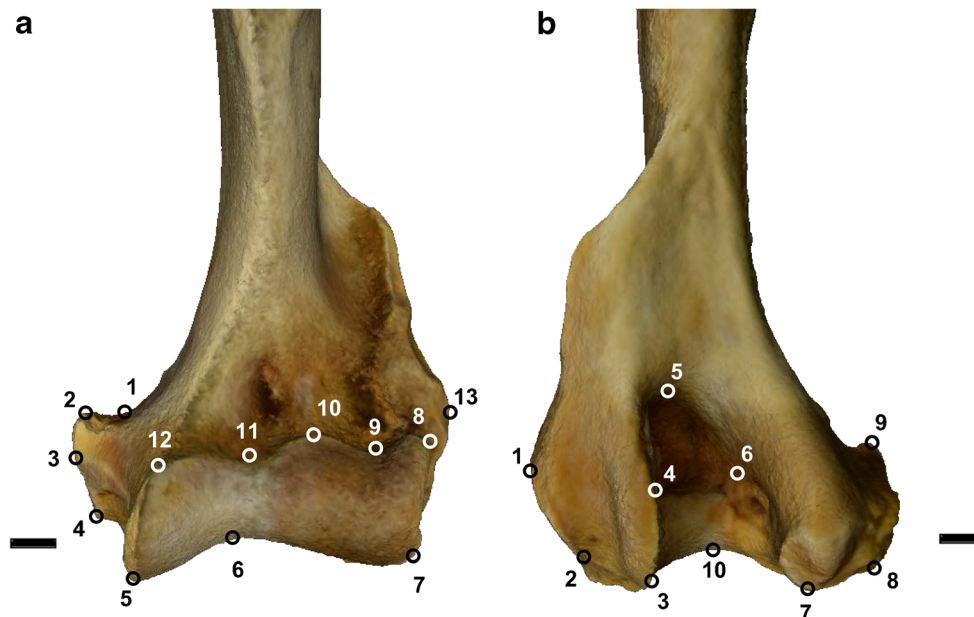


Fig. 1 Two dimensional landmarks positioned on the elbow joint in (a) cranial and (b) caudal views of a specimen of *Tremarctos ornatus*. For (a) landmarks are defined as follow: 1, limit between medial epicondyle and entepicondylar bar; 2, highest point of the medial epicondyle; 3, lowest point of the medial epicondyle; 4, lowest point on the groove between landmarks 3 and 5; 5, medial end of trochlea distally; 6, distal junction between the trochlea and capitulum; 7, most distal and most lateral point of the capitulum; 8, most proximal and most lateral point of the capitulum; 9, lowest point on proximal surface of the capitulum; 10, highest point between landmarks 9 and 11; 11, proximal junction

between the trochlea and capitulum; 12, medial end of trochlea proximally; 13, most lateral point on the lateral epicondyle. For (b) landmarks are defined as follow: 1, most lateral point on the lateral epicondyle; 2, maximum curvature point between landmarks 1 and 3; 3, most distal and lateral point of the capitulum; 4, most proximal and lateral point on the capitulum; 5, proximal tip of the olecranon fossa; 6, most proximal and medial point on the capitulum; 7, distal tip of the trochlea; 8, maximum curvature point between landmarks 7 and 9; 9, upper point on the medial epicondyle; 10, distal junction between trochlea and capitulum. Scale bar is equal to 1 cm

for cranial and caudal views of the elbow joint (Rohlf and Slice 1990). The new set of coordinates (=Procrustes coordinates; Proc) were subjected to principal component analysis (PCA) in order to identify major patterns of variation between specimens. By using thin-plate spline, shape variation from the mean configuration was visualized for each principal component axis (named in this case Relative Warp; RW). The software tpsRelw 1.53 was employed to extract centroid size, procrustes aligned coordinates, and relative warp scores (Rohlf 2015).

We employed Procrustes ANOVA, non-parametric Multivariate Analysis of Variance (MANOVA), and one-way ANOVA to test for differences between genera and species in elbow joint shape and size (= natural log transformed CS). As sex was available for a limited number of species and specimens ($N = 24$ of which 12 were females and 12 males; Table 1), we were not able to perform any robust assessment of sexual dimorphism in our sample, which for this particular study was not taken into account. All the analyses were performed using PAST and the R package geomorph (Adams and Otárola-Castillo 2013).

Paleobiological Predictions

In order to provide paleobiological insights into Quaternary fossil specimens, all extant bear taxa (except the hybrid specimen *U. arctos* x *U. maritimus*) were categorized according to their locomotory behavior and habitat adaptations (Table 1).

Ortolani and Caro (1996) claimed for all the bears the possibility of being ‘Terrestrial but Climbs’ with the exception of the polar bear (*Ursus maritimus*) considered ‘Aquatic’. Later attempts by Samuels et al. (2013) also provided classification of bears into terrestrial, scansorial, and semiaquatic categories. Here, we opted to categorize extant species according to their degree of arboreality as in Iwaniuk et al. (2000). Based on this classification, all extant bears have a good degree of arboreality scoring (scored 2 = semiarboreal) with the exception of *Ursus arctos* (scored 1 = scansorial; only juveniles generally climb, with big adults never observed doing so consistently) and the polar bear (scored 0 = incapable of climbing). This classification was supported by multiple references from different authors that included behavioral observations of wild and captive individuals (see Iwaniuk et al. 2000).

For habitat adaptations, we employed the same methodology as in Meloro et al. (2013) using the general categorization of Ortolani and Caro (1996) as a starting point. Each species was scored according to its presence in different broad habitat types that include: temperate forest and tropical forest [closed], grassland and arctic [open] (riparian was discarded). Accordingly, the giant panda (*Ailuropoda melanoleuca*), the sun bear (*Helarctos malayanus*), the sloth bear (*Melursus ursinus*), and the Asiatic black bear (*Ursus thibetanus*) are

categorized as ‘closed’; brown bear (*Ursus arctos*), American black bear (*Ursus americanus*), and spectacled bear (*Tremarctos ornatus*) are ‘mixed’, while the polar bear (*Ursus maritimus*) is classified as ‘open’.

Discriminant function analysis (DFA) was applied using ecological categorizations as factors and Procrustes coordinates and size (=LnCS) as predictors. As proposed in Meloro (2011b), Meloro and Louys (2015), and Meloro et al. (2013, 2015), a stepwise variable selection allows to minimize number of predictors in DFA avoiding overfitting of categorical differences. Variables selected by DFA models had F value with $p > 0.05$; variables removed had $p < 0.10$. Efficacy of discriminant functions in categorizing fossil taxa was assessed using jack-knife cross validation classification rate (Kovarovic et al. 2011). The software IBM SPSS statistics version 23 was employed to generate DFA models.

As cranial and caudal views are elements of the same structure, we employed two blocks Partial Least-Squares (PLS) to test the hypothesis that their shape co-varies (Rohlf and Corti 2000; Fabre et al. 2014). PLS was also re-performed on specimens grouped by size classes (a small class that includes all the semiarboreal extant bears, and a large one that includes brown, polar, and fossil bears) to test the hypothesis that size and climbing ability might influence co-variation patterns in the elbow joint. Differences in covariation trajectories between the two classes were tested using angular comparison of the PLS vectors (Klingenberg and Marugán-Lobón 2013). The PLS analyses were complementarily performed using tpsPLS (Rohlf 2015) and MorphoJ (Klingenberg 2011).

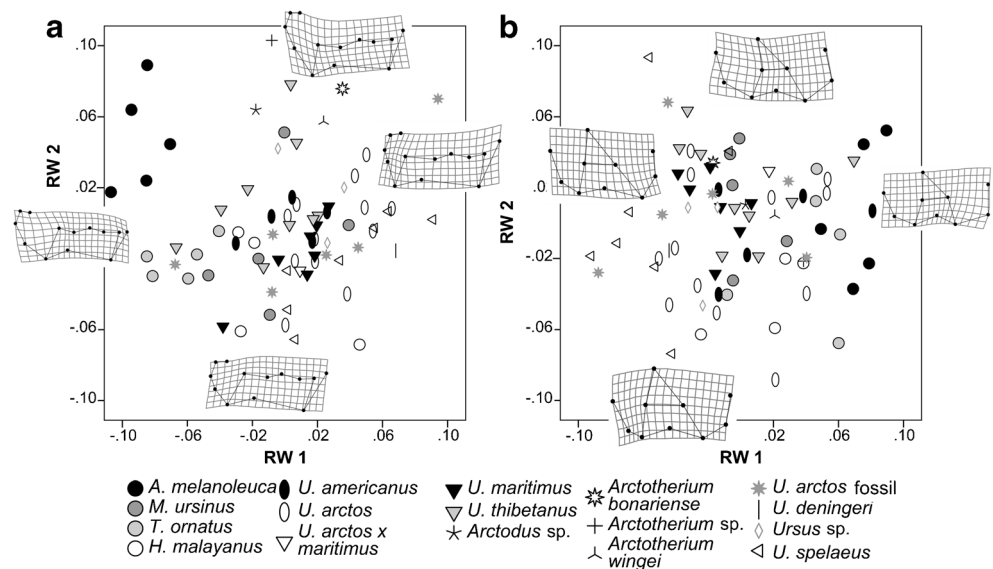
The 2D data generated for this study (including centroid size, procrustes aligned coordinates, and relative warp scores) are all available in Appendix 1.

Results

Taxonomy

A relative warp analysis of the cranial view extracted 22 RW vectors of which the first fourteen explained almost 95% of total variance (=94.63% var.). A plot of RW1 (26.12% var.) vs RW2 (17.42% var.) showed a discrete degree of separation between extant species, with the giant panda and the sun bear occupying the most negative RW1 scores, while the brown bear the most positive (Fig. 2). Along this vector were major shape changes related to the expansion of the trochlea relative to the medial epicondyle (that is shorter on RW1 positive scores and broader on RW1 negative scores). On the second axis, there was a proximo-distal enlargement of the medial epicondyle (wider for positive scores occupied and narrower for negative scores) relative to the trochlea (Fig. 2). In the caudal view, 95% var. was explained by the first 12 RWs (out of 16). RW1 (20.78% var.) described shape changes in

Fig. 2 Relative warp plots describing the scatter of specimens across RW1 and RW2. In **a**, the plot represents cranial view of the elbow joint, in **b**, the caudal view. Transformation grids, at the extremes of each RW axis, show the relative deformation from the mean shape. Landmarks are linked by a wireframe in all transformation grids and specimens are labelled according to species



both medial and lateral epicondyles, with negative scores being occupied by cave bears (*Ursus spelaeus*) while the giant panda was on positive scores with larger lateral epicondyle (Fig. 2). On RW2 (14.70% var.), the olecranon fossa was relatively expanded on negative scores and contracted on positive scores. No discrimination among taxa was evident using caudal shape RW scores.

Procrustes ANOVA demonstrated that significant differences between genera (including both extant and fossils) occurred in both cranial ($F = 4.984$, $Z = 3.676$, $df = 6, 67$, $P < 0.0001$; $r^2 = 0.308$) and caudal shape ($F = 2.390$, $Z = 2.110$, $df = 6, 67$, $P < 0.0001$; $r^2 = 0.177$). In order to test for species differences, a number of fossil specimens were removed and Quaternary *Ursus arctos* was considered as a separate taxon. A non-parametric MANOVA showed that in cranial view species are significantly different in shape ($Tot SS = 0.4765$, $Within-group SS = 0.2886$, $F = 4.05$, $P < 0.0001$) with both the giant panda and *T. ornatus* being mostly different from all the other species (Table 2). In caudal view, species were equally distinct in shape ($Tot SS = 0.5648$, $Within-group SS = 0.4049$, $F = 2.458$, $P < 0.0001$) with the giant panda again showing the highest degree of distinctiveness (Table 3).

Size and Allometry

There were significant differences between species in natural log transformed centroid size for both cranial ($F = 15.986$, $df = 11, 59$, $P < 0.001$) and caudal views of the elbow joint ($F = 11.393$, $df = 11, 59$, $P < 0.0001$; Fig. 3). Post-hoc tests showed *Arctotherium* specimens (grouped altogether for this analysis) being significantly larger than all bear species (all $P < 0.05$) except fossil *U. arctos* ($P = 0.086$), and cave bears ($P = 0.249$) in cranial view. Among extant species, the polar bear was generally the largest species. No significant

differences were detected between *U. maritimus* and *U. arctos* (both extant, $P = 0.097$ and fossils $P = 1.00$), and cave bears ($P = 0.958$). In caudal view, size differences were less pronounced with *Helarctos malayanus* emerging for being significantly smaller than extant and fossil brown, polar, and cave bears ($P < 0.01$). Among the fossil species, the cave bears are significantly the largest although they showed no differences from the polar bear ($P = 0.761$), the fossil brown bear ($P = 1.00$) and the *Arctotherium* spp. ($P = 0.978$).

Size significantly influenced elbow joint shape (cranial: $Wilk's \lambda = 0.444$; $F_s = 2.903$, $df = 22, 51$, $P < 0.0001$; caudal: $Wilk's \lambda = 0.464$; $F_s = 4.109$, $df = 16, 57$, $P < 0.0001$) explaining 4.776 and 5.63% of shape variance in cranial and caudal views, respectively (Fig. 3). Deformation grids demonstrated that large bears are characterized by a relatively wider and lower trochlea together with a shorter epicondylar region, while in caudal view the olecranon fossa was significantly smaller (Fig. 3).

Locomotion

In cranial view, one-way ANOVA demonstrated that size differs significantly between locomotory categories ($F = 22.127$, $df = 2, 49$, $P < 0.001$). Locomotion explained a substantial portion of joint size variation ($r^2 = 0.453$). An equivalent Procrustes ANOVA confirmed that locomotion categories differed also in the shape of the joint in cranial view ($F = 3.3414$, $Z = 2.8985$, $df = 2, 49$, $P < 0.0001$), although the variance explained is much lower ($r^2 = 0.120$).

The stepwise DFA model extracted two significant functions loaded on six variables, including LnCS, and five Procrustes coordinates (Table 4). Discriminant Function 1 (DF1; $Wilk's \lambda = 0.160$, $\chi^2 = 85.239$, $df = 12$, $P < 0.0001$) explained 85.24% of variance; DF2 ($Wilk's \lambda = 0.645$,

Table 2 Probability values for post-hoc comparisons after non-parametric MANOVA models performed on RW scores of elbow joint cranial view

	<i>A. melanoleuca</i>	<i>H. malayanus</i>	<i>M. ursinus</i>	<i>T. ornatus</i>	<i>U. americanus</i>	<i>U. arctos</i>	<i>U. arctos fossil</i>	<i>U. maritimus</i>	<i>U. spelaeus</i>	<i>U. thibetanus</i>
<i>A. melanoleuca</i>	–	0.342	0.383	0.383	0.374	0.005	0.032	0.050	0.054	0.032
<i>H. malayanus</i>	0.008	–	0.365	0.306	1.000	0.153	0.428	1.000	0.252	0.351
<i>M. ursinus</i>	0.009	0.008	–	0.410	1.000	0.032	1.000	0.248	1.000	1.000
<i>T. ornatus</i>	0.009	0.007	0.009	–	0.324	0.005	0.090	0.059	0.041	0.018
<i>U. americanus</i>	0.008	0.193	0.024	0.007	–	1.000	1.000	1.000	0.045	1.000
<i>U. arctos</i>	0.000	0.003	0.001	0.000	0.131	–	1.000	1.000	0.005	0.032
<i>U. arctos fossil</i>	0.001	0.010	0.478	0.002	0.092	0.031	–	1.000	1.000	1.000
<i>U. maritimus</i>	0.001	0.137	0.006	0.001	0.381	0.117	0.153	–	0.027	0.752
<i>U. spelaeus</i>	0.001	0.006	0.051	0.001	0.001	0.000	0.193	0.001	–	0.018
<i>U. thibetanus</i>	0.001	0.008	0.037	0.000	0.761	0.001	0.120	0.017	0.000	–

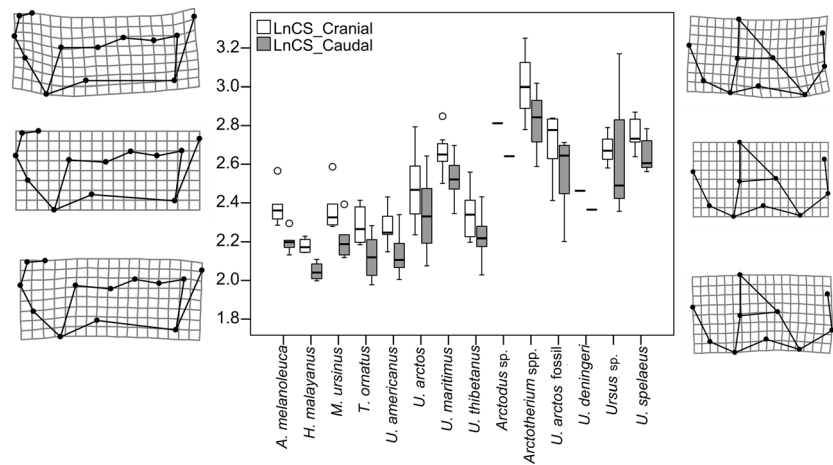
P values above diagonal are modified after Bonferroni correction. Significant *P* values (< 0.05) are in bold

Table 3 Probability values for post-hoc comparisons after non-parametric MANOVA models performed on RW scores of elbow joint caudal view

	<i>A. melanoleuca</i>	<i>H. malayanus</i>	<i>M. ursinus</i>	<i>T. ornatus</i>	<i>U. americanus</i>	<i>U. arctos</i>	<i>U. arctos fossil</i>	<i>U. maritimus</i>	<i>U. spelaeus</i>	<i>U. thibetanus</i>
<i>A. melanoleuca</i>	–	1.000	0.275	0.342	0.756	0.032	0.225	0.054	0.068	0.072
<i>H. malayanus</i>	0.026	–	0.432	1.000	1.000	1.000	1.000	0.216	0.405	0.698
<i>M. ursinus</i>	0.006	0.010	–	0.446	1.000	1.000	1.000	1.000	0.873	1.000
<i>T. ornatus</i>	0.008	0.119	0.010	–	1.000	1.000	0.171	0.036	0.270	0.572
<i>U. americanus</i>	0.017	0.251	0.102	0.290	–	1.000	1.000	0.059	1.000	1.000
<i>U. arctos</i>	0.001	0.165	0.287	0.024	0.172	–	1.000	0.617	1.000	1.000
<i>U. arctos fossil</i>	0.005	0.024	0.696	0.004	0.067	0.211	–	0.698	1.000	1.000
<i>U. maritimus</i>	0.001	0.005	0.040	0.001	0.001	0.014	0.016	–	1.000	1.000
<i>U. spelaeus</i>	0.002	0.009	0.019	0.006	0.025	0.024	0.059	0.031	–	1.000
<i>U. thibetanus</i>	0.002	0.016	0.410	0.013	0.265	0.100	0.090	0.098	0.112	–

P values above diagonal are modified after Bonferroni correction. Significant *P* values (< 0.05) are in bold

Fig. 3 Box plot showing differences in natural log transformed centroid size (LnCS) between extant and fossil species of ursid elbow joint. Data from cranial view are presented in white boxes, while data from caudal view in grey. Elbow joint shape deformation are showed laterally to represent size-related variation from the smallest to the largest specimen in cranial (left) and caudal (right) view



$\chi^2 = 20.410$, $df = 5$, $P = 0.001$) explained 15.4% var. and was highly correlated with size. A plot of the discriminant scores (Fig. 4a) showed a good degree of discrimination between locomotory groups with semiarboreal specimens particularly well separated on positive DF1 scores and characterized by a relatively shorter and wider trochlea and a wider medial epicondyle. This was confirmed by percentages of correctly classified cases after cross-validation (total of 84.8%; Table 5). Applying these functions allowed to predict a non-climbing ability for all fossil specimens (including the American genera *Arctotherium* and *Arctodus*) except some *Ursus arctos*, *U. deningeri*, and one *U. spelaeus*, which were categorized as scansorial (Table 6). The hybrid brown x polar

bear was equally categorized as scansorial. Excluding the category of non-climbing (represented by the polar bear alone) allowed extracting one significant DF1 (*Wilk's* $\lambda = 0.344$, $\chi^2 = 43.732$, $df = 4$, $P < 0.0001$) loaded on four Procrustes coordinates but not on size (Table 4). Classification rates increased for the semiarboreal category (Table 5), still with the brown x polar bear hybrid and the majority of fossils being categorized as scansorial with few exceptions (Table 6).

In caudal view, the natural log transformed centroid size averages also differed between locomotory categories ($F = 24.322$, $df = 2$, 49 , $P < 0.001$), which explained almost half of the size variation ($r^2 = 0.498$). Differences in shape were again confirmed by Procrustes ANOVA ($F = 2.1083$,

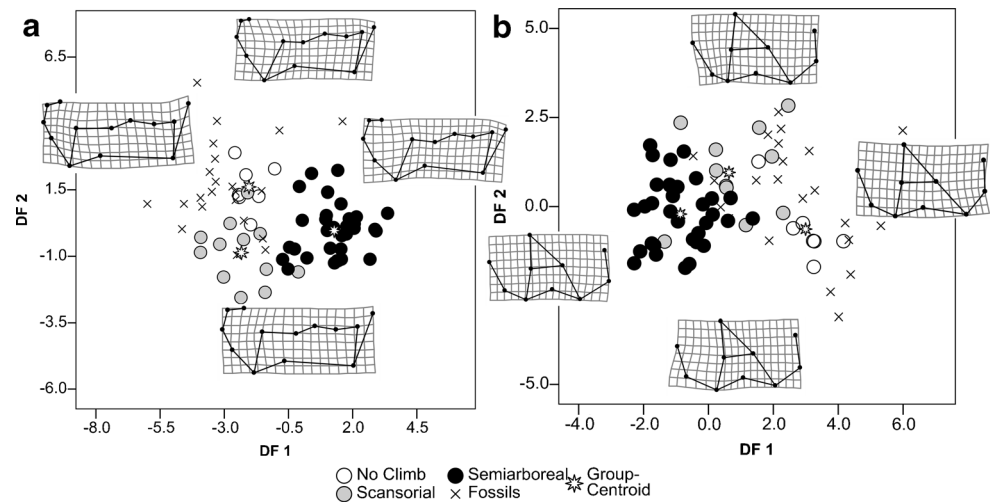
Table 4 Loadings of different discriminant function vectors based on natural log transformed centroid size and a selection of Procrustes coordinates (being a bi-dimensional system they are divided into X and Y) after stepwise procedure

	Cranial view						Caudal view					
	Locomotion		Loc NoP	Habitat		Hab NoP	Locomotion		Loc NoP	Habitat		Hab NoP
	DF1	DF2	DF1	DF1	DF2	DF1	DF1	DF2	DF1	DF1	DF2	DF1
LnCS	-0.467	0.663	-	0.465	0.683	-	0.724	0.140	0.622	-0.626	0.204	-
Proc 1X	-0.286	-0.388	-0.424	-	-	-	/	/	/	/	/	/
Proc 2X	/	/	/	/	/	/	0.125	0.869	0.600	-	-	-
Proc 2Y	0.095	-0.017	-	-0.317	0.255	0.35	/	/	/	/	/	/
Proc 6Y	0.092	0.192	0.155	-	-	-	-	-	-	0.188	-0.267	-
Proc 7X	-	-	-	0.193	-0.354	-	0.338	-0.030	-	-	-	-
Proc 7Y	/	/	/	/	/	/	0.152	-0.188	-	-	-	-
Proc 8X	/	/	/	/	/	/	/	/	0.164	-	-	-
Proc 8Y	0.170	0.023	0.195	-0.353	0.24	0.372	-	-	-	0.107	-0.549	-
Proc 9Y	-	-	-	-	-	0.187	-	-	-	0.137	0.97	1.00
Proc 12X	0.356	0.213	0.466	-	-	-	/	/	/	/	/	/
Proc 12Y	-	-	-	-	-	0.231	/	/	/	/	/	/
Proc 13X	-	-	-	0.269	-0.337	-	/	/	/	/	/	/

Values in bold indicate the largest absolute correlation between a variable and discriminant function vector 1 or 2

Abbreviations: Loc NoP = Locomotion excluding polar bear, Hab NoP = Habitat excluding polar bear, Proc = Procrustes coordinates

Fig. 4 Scatter plots of the first two discriminant functions (DF) extracted from a combination of shape and size variables to predict locomotory adaptations in (a) cranial and (b) caudal views of the elbow joint. Extant specimens are labelled according to their locomotion. Fossil specimens are labelled as crosses. Deformation grids demonstrate variation from the most negative to the most positive DF scores and were obtained by regressing original shape coordinates vs DF vector scores



$Z = 1.9365$, $df = 2$, 49 , $P = 0.0034$) with a much lower variance explained ($r^2 = 0.0792$). DFA produced two discriminant functions loaded on five variables inclusive of centroid size. DF1 (85.9% var., $Wilk's \lambda = 0.265$, $\chi^2 = 63.136$, $df = 8$, $P < 0.0001$) was positively loaded on size and Procrustes coordinate 7X, while DF2 (14.1% var., $Wilk's \lambda = 0.763$, $\chi^2 = 12.819$, $df = 3$, $P = 0.005$) was loaded positively on Procrustes coordinate 2X and negatively on 7Y (Table 4). Plotting the two functions showed the semi-arboreal specimens to be characterized by a relatively wider medial epicondyle compared to the non-climbers (Fig. 4b). There was a similar performance of DFA classification accuracy compared to the cranial view, although on the caudal view percentages dropped for the non-climbing category (Table 5). The majority of fossil specimens were categorized as non-climbers with the exception of *Arctotherium* sp., *Arctodus* sp., and different species of *Ursus* (Table 6). The brown x polar bear hybrid was validated as scansorial. After the exclusion of the polar bear specimens, DFA extracted one function ($Wilk's \lambda = 0.556$, $\chi^2 = 24.342$, $df = 3$, $P = 0.001$) loaded on size and two

Procrustes coordinates only. Classification accuracy improved for scansorial specimens (Table 5) with the hybrid specimen and most of the fossils being predicted within this category (Table 6).

Habitat

Based on cranial view, centroid size differed across habitat categories ($F = 14.525$, $df = 2$, 49 , $P < 0.0001$) and explained a relatively high proportion of shape variation ($r^2 = 0.372$). Shape also differed significantly between habitat categories ($F = 3.114$, $Z = 2.078$, $df = 2$, 50 , $P = 0.0061$), which explained 8% of shape variation ($r^2 = 0.085$). DFA selected five variables capable of discriminating habitat categories based on the cranial view. DF1 (75.8% var., $Wilk's \lambda = 0.251$, $\chi^2 = 64.988$, $df = 10$, $P < 0.0001$) was loaded on two Procrustes coordinates, while DF2 ($Wilk's \lambda = 0.658$, $\chi^2 = 19.651$, $df = 4$, $P = 0.001$) correlated significantly also with LnCS (Table 4). Bears from closed habitats showed a wider trochlea and a broader medial epicondyle (Fig. 5a)

Table 5 Percentage of classified cases for each ecological category after performing leave one out procedure on discriminant function models based on natural log centroid size and Procrustes coordinates as independent variables selected with stepwise procedure

		No Climb	Scansorial	Semi-arboreal	Open	Mixed	Closed	
Cranial view	No Climb	85.7	14.3	0.0	85.7	14.3	0.0	Open
	Scansorial	8.3	83.3	8.3	13.6	68.2	18.2	Mixed
	Semi-arboreal	6.1	9.1	84.8	4.3	13.0	82.6	Closed
Caudal view	No Climb	85.7	14.3	0.0	100.0	0.0	0.0	Open
	Scansorial	16.7	66.7	16.7	18.2	45.5	36.4	Mixed
	Semi-arboreal	0.0	18.2	81.8	0.0	39.1	60.9	Closed
Cranial view	Scansorial		83.3	16.7		81.8	18.2	Mixed
	Semi-arboreal		12.1	87.9		17.4	82.6	Closed
Caudal view	Scansorial		75.0	25.0		77.3	22.7	Mixed
	Semi-arboreal		21.2	78.8		43.5	56.5	Closed

Percentages in bold indicate the correct classification for each category while the other values indicate percentage of misclassifications

Table 6 Locomotory and habitat categorical predictions for fossil bears based on a different number of DFA models

Fossil specimens	Cranial view				Caudal view			
	Locomotion	Loc. No Polar	Habitat	Hab. No Polar	Locomotion	Loc. No Polar	Habitat	Hab. No Polar
<i>Arctotherium</i> sp. UFMS (Bodoquena Plateau)	No Climb	Scansorial*	Open*	Mixed	Scansorial*	Scansorial	Open*	Closed
<i>Ursus</i> sp. NHM 21287a (Grays, Essex)	No Climb^	Scansorial	Open^	Closed	No Climb^	Scansorial	Open^	Closed
<i>Ursus arctos</i> NHM 48744 (Brixton Cave)	Scansorial*	Scansorial	Mixed^	Closed	Scansorial*	Scansorial	Closed^	Mixed
<i>Ursus arctos</i> NHM M41273 (Devon)	Semiarboreal^	Semiarboreal	Closed*	Closed	Scansorial^	Scansorial	Closed	Closed
<i>Ursus arctos</i> NHM M41277 (Devon)	Scansorial*	Scansorial	Open	Mixed*	Scansorial*	Scansorial	Mixed	Closed
<i>Ursus arctos</i> NHM M4129 (Tormenton cave)	No Climb^	Semiarboreal	Open*	Mixed	No Climb^	Semiarboreal	Open*	Closed
<i>Ursus arctos</i> NHM TNXVIIC5B1960 (Tormenton cave)	No Climb^	Scansorial	Open^	Closed	No Climb^	Scansorial	Open^	Closed
<i>Ursus arctos</i> NHM TNXXI5B1957 (Tormenton cave)	No Climb^	Scansorial	Open*	Mixed	No Climb^	Scansorial	Open	Closed
<i>Ursus deningeri</i> NHM M968 (Kent's cavern)	Scansorial*	Scansorial	Mixed*	Mixed*	Scansorial*	Semiarboreal	Mixed*	Mixed*
<i>Ursus spelaeus</i> NHM M3551 (Cave Jerzmanowice Alkurz)	No Climb*	Semiarboreal	Open*	Closed	No Climb*	Scansorial	Open*	Mixed
<i>Ursus</i> sp. NHM 21287 (Grays, Essex)	No Climb^	Semiarboreal	Open*	Mixed	Scansorial^	Scansorial^	Open*	Closed
<i>Ursus</i> sp. NHM 23137 (Grays, Essex)	Scansorial*	Scansorial	Open	Mixed*	Scansorial*	Semiarboreal	Mixed*	Mixed*
<i>Arctodus</i> sp. MNHN NUA10 (unknown)	No Climb^	Semiarboreal	Open	Mixed*	Scansorial^	Scansorial	Mixed*	Closed
<i>Arctotherium bonariense</i> MNHN PAM552 (near Lujan)	No Climb*	Semiarboreal	Open*	Mixed	No Climb*	Scansorial	Open*	Closed
<i>Arctotherium wingei</i> MNHN PAM547 (unknown)	No Climb*	Semiarboreal	Open	Mixed	No Climb*	Scansorial	Open*	Closed
<i>Ursus spelaeus</i> MNHN SN0 (unknown)	No Climb^	Semiarboreal	Open^	Closed	Scansorial*	Scansorial*	Mixed^	Mixed^
<i>Ursus spelaeus</i> MNHN SN1 (unknown)	No Climb*	Semiarboreal	Open^	Mixed	No Climb*	Scansorial	Open^	Mixed
<i>Ursus spelaeus</i> MNHN SN2 (unknown)	No Climb^	Semiarboreal	Open^	Mixed	No Climb^	Semiarboreal	Open^	Mixed
<i>Ursus spelaeus</i> MNHN SN3 (unknown)	No Climb	Scansorial*	Open^	Mixed	Scansorial*	Scansorial	Open^	Mixed
<i>Ursus spelaeus</i> MNHN SN4 (unknown)	NoClimb^	Scansorial	Open^	Mixed	No Climb^	Scansorial	Open^	Mixed
<i>Ursus spelaeus</i> MNHN SN5 (unknown)	No Climb^	Scansorial	Open^	Closed	No Climb^	Scansorial	Open^	Mixed

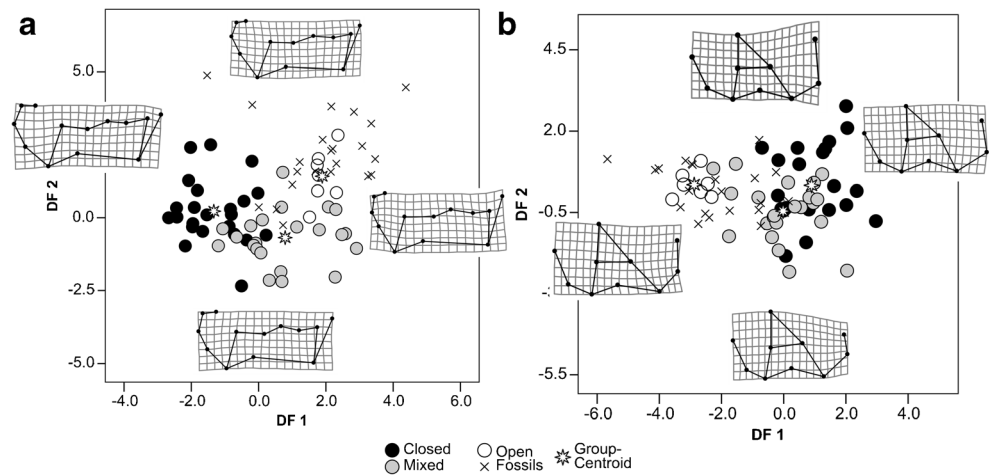
The symbol * represented the commonest and most likely prediction, while the symbol ^ is for categories with highest percentage of accuracy prediction

while many fossils clustered on positive DF1 scores within the group of open habitat. Percentage of correct re-classification is relatively lower when compared to locomotion categories and confirmed the attribution of the majority of fossils to ‘open’ with few exceptions, including the hybrid brown × polar bear classified as ‘mixed’ (Table 6). Excluding the polar bear, showed one significant DF1 (*Wilk's* $\lambda = 0.389$, $\chi^2 = 37.782$, $df = 6$, $P < 0.0001$) loaded on five coordinates (Table 4). Classification accuracy improved for mixed habitat and remained the same for ‘closed’ (Table 5). Many fossils *Ursus* were classified as ‘closed’ while all *Arctotherium* and *Arctodus* were ‘mixed’ (Table 6).

Averaged centroid size in caudal view differed across habitat categories ($F = 15.134$, $df = 2, 49$, $P < 0.0001$), which explained almost 40% of variation ($r^2 = 0.382$). Procrustes ANOVA confirmed differences in shape ($F = 1.6545$, $Z = 1.547$, $df = 2, 50$, $P = 0.0036$), although with small amount of variation explained ($r^2 = 0.062$). Discriminant functions

were equally loaded on size and four Procrustes variables. DF1 was significant (90.5% var., *Wilk's* $\lambda = 0.335$, $\chi^2 = 51.88$, $df = 8$, $P < 0.0001$) and loaded negatively on size (Table 4), while DF2 was not significant (9.5% var., *Wilk's* $\lambda = 0.859$, $\chi^2 = 7.222$, $df = 3$, $P = 0.065$). Scatterplot showed significant overlap between ‘closed’ and ‘mixed’, with a separated group for ‘open’ specimens characterized by wide trochlea and relatively short medial epicondyle. Classification accuracy is 100% for open but below 50% for ‘mixed’ (Table 5). The brown × polar bear hybrid was consistently classified as ‘mixed’. The majority of fossils are classified as ‘open’, with *Arctodus* sp. and *U. deningeri* as ‘mixed’ and a number of fossil *Ursus* as ‘closed’ (Table 6). The exclusion of the polar bear generated one significant DF (*Wilk's* $\lambda = 0.842$, $\chi^2 = 7.330$, $df = 1$, $P = 0.007$), which improved classification accuracy for ‘mixed’ but not for ‘closed’ (Table 5). This function was loaded on one coordinate only and predicted the majority of fossils as ‘closed’ (including the

Fig. 5 Scatter plots of the first two discriminant functions (DF) extracted from a combination of shape and size variables to predict habitat adaptations in (a) cranial and (b) caudal views of the elbow joint. Extant specimens are labelled according to their habitat preference. Fossil specimens are labelled as crosses. Deformation grids demonstrate variation from the most negative to the most positive DF scores and were obtained by regressing original shape coordinates vs DF vector scores



extant brown x polar bear hybrid) except the cave bears (Table 6).

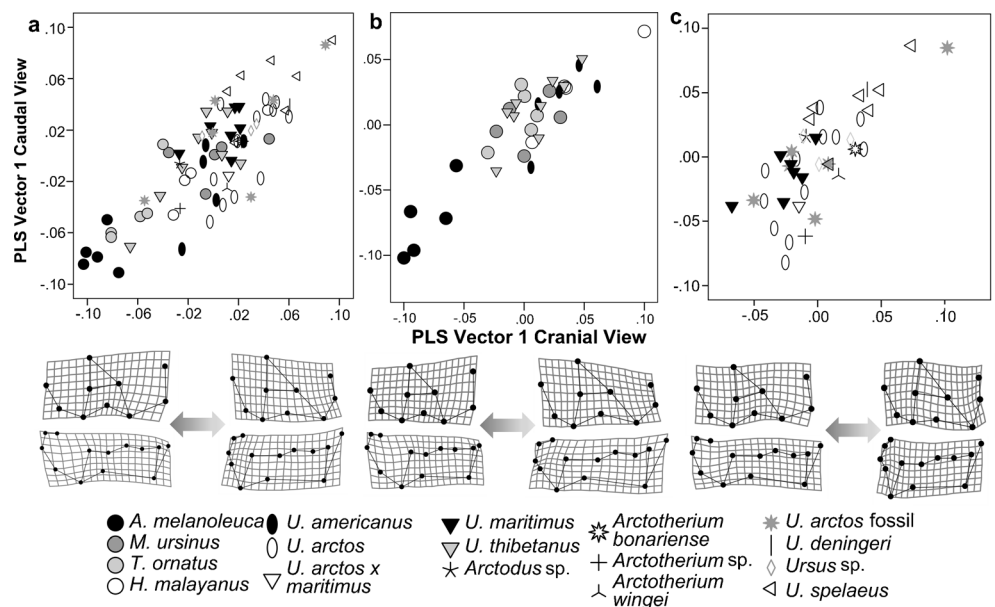
Covariation Patterns

Two blocks PLS identified sixteen pairs of vectors of which the first pair explained 60.18% of covariation between shape of the cranial and caudal views. There was a highly significant correlation (RV coefficient = 0.464, $r = 0.82$, $P < 0.0001$; Fig. 6a) between the cranial and caudal PLS1 vector scores. On the negative scores, the giant panda specimens are characterized by an expanded medial epicondyle evident in both cranial and caudal view and a relatively elongated trochlea. At the extreme positive, the large cave bears and fossil *U. arctos* showed a shorter medial epicondyle and a wider trochlea. Centroid size significantly influenced PLS1 vector

scores on both cranial (Pearson $r = 0.415$, $P < 0.0001$) and caudal views (Pearson $r = 0.457$, $P < 0.0001$).

In small, semiarborescent bears, the degree of covariation between the cranial and caudal views was much stronger (RV coefficient = 0.645, PLS1 $r = 0.91$, $P < 0.0001$; Fig. 6b) than in larger taxa (RV coefficient = 0.349, PLS1 $r = 0.75$, $P < 0.0035$; Fig. 6c). Deformation grids showed that in small bears as the trochlea becomes (from negative to positive scores) wider and longer, the olecranon region also expands its articular surface (Fig. 6b). Conversely, in large bears expansion of the olecranon area (from negative to positive scores) corresponds to a shortening and widening of the trochlea (Fig. 6c). This pattern is confirmed by an angle of 72.51 degrees ($P = 0.157$) on PLS1 vector cranial view evidencing substantial differences in the integration trajectories between small and large bears. The same applies for PLS1 vector caudal view with an angle of 72.979 degrees ($P = 0.254$). Size did

Fig. 6 Scatter plot of the first pair of Partial Least Squares vectors depicting degree of covariation between cranial and caudal view shape data of ursid elbow joint. Below each scatter plot deformation grids show how covariation in both structures occur from the most negative (left side) towards the most positive (right side) scores. In a, all bear specimens are included in the analyses while in b, a subsample of small ($N = 33$) semiarborescent taxa is presented. In c, all large specimens ($N = 41$) are presented including fossils



not significantly correlate with any PLS vector in small bears, while it did for large ones (size vs PLS1 cranial: *Pearson* $r = 0.339$, $P = 0.030$; size vs PLS1 caudal: *Pearson* $r = 0.339$, $P < 0.0001$).

Discussion

The elbow joint of bears is no exception among Carnivora for being a bony element that brings insights into taxonomy, locomotion, and habitat adaptation. In keeping with previous similar attempts (i.e., Walmsley et al. 2012 on felids), we identified a strong component of variation in elbow joint size and shape due to genus and species differentiation. Both cranial and caudal views showed taxonomic distinctiveness in size and shape for the majority of extant species with the giant panda (*Ailuropoda melanoleuca*) being the most unique in morphology (Fig. 2; Tables 2 and 3). This confirms early descriptions by Davis (1964) that highlighted for the giant panda the presence of a particularly enlarged epicondyle region. As for *Tremarctos ornatus* this character relates to the presence of the foramen epicondylaris, which transmits the median nerve and the ulnar artery. The relative warp plots (Fig. 2) show in both cranial and caudal views the giant panda and *Tremarctos* specimens at the extreme of RW1 scores, confirming this empirical observation. The same plots highlighted a degree of overlap between *Ursus* species with cave bears that generally occupy the extreme RW1 score opposite to the giant panda (see Fig. 2b). The non-parametric MANOVA confirmed lack of differentiation in elbow joint shape for the polar bear and fossil *Ursus arctos* (Tables 2 and 3). Cave bears are more distinguishable in the shape of the cranial but not the caudal view and the same applies to the brown bear and the Asiatic black bear. Members of the American genera *Arctodus* and *Arctotherium* occupied extreme positive RW2 scores in the cranial view because of their expanded medial epicondyle, although in caudal view they overlapped with *Ursus* species (Fig. 2a, b). Such discrepancies in discriminatory power were observed also with different datasets (Walmsley et al. 2012) and they might relate to the significance and complexity of the trochlea region (Andersson and Werdelin 2003; Andersson 2004), which is better captured by the cranial view.

When ecological adaptations are concerned, the cranial view again appears to be more informative than the caudal view (see Table 5). It is apparent that size is a much more informative trait than shape in this particular case, as the variance explained by locomotion and habitat is much higher (ranging from 37 to 50% compared to 6–12% in shape). The ability to climb in extant bears seems to be broadly constrained by body mass since in the brown bear (*Ursus arctos*) it is almost lost from the juvenile to the adult (Iwaniuk et al. 2000). This observation forces inferences on

Quaternary fossils, which are in general much larger than extant species (Fig. 3). It is intuitive to believe that at large body size climbing ability – but not forelimb dexterity (Iwaniuk et al. 2000) – reduces in mammals in general. Consequently, size was not discarded by most of the discriminant function models to predict locomotion as well as habitat. The inclusion of size as an ecological predictor in geometric morphometric data on Carnivora has been highlighted by Meloro (2011b) and Meloro et al. (2015). Our study adds evidence to the already well established paradigm that body mass in Carnivora interacts strongly with ecology (Gittleman 1985), and does not need to be discarded a priori in the analyses of their functional morphology. The predictive accuracy of most DFA models decreased consistently in both cranial and caudal views when the polar bear was excluded and size was not stepwise selected (Table 5).

The classification provided for the hybrid brown x polar bear is consistent with our visual inspection of the morphology of this specimen, which resembles much more brown than polar bear both in skull and postcranial features (Meloro pers. obs.). Preuß et al. (2009) recently reported observation of two captive hybrids whose head morphology appears to resemble brown more than polar bears. In our results the occurrence of a dominant phenotype in the skeleton of hybrid bears, although more morphological, in conjunction with molecular data, are necessary to establish a pattern of variation.

In the majority of cases, fossil brown bears and cave bears are consistently categorized like the polar bear as lacking the ability of climbing and adapted to open habitats. The same applies for the American genera *Arctodus* and *Arctotherium*, although the exclusion of the polar bear provides contrasting evidences (Table 6). Based on the lower discriminatory power of the caudal view of the joint, we can confidently discard possibilities for the American fossil bears of being adapted to a closed environment while the habitat categories ‘open’ and ‘mixed’ seem compatible with previous paleoecological attempts. Figueirido et al. (2010) reported for *Arctodus simus* lack of predatory adaptations in the long bones and an omnivorous diet, which has also been proposed for *Arctotherium* species in general (Prevosti and Vizcaíno 2006; Figueirido and Soibelzon 2010; Prevosti and Martin 2013; Soibelzon et al. 2009; 2014). Arnaudo et al. (2016) proposed for *Arctotherium tarijense* an increased ability to cope with a variety of environments based on the inner ear morphology thus supporting our predicted mixed categorization also for the other *Arctotherium* species. This result still should be considered with caution because intra- and interspecific variation of inner ear morphology is broad in bears (Arnaudo et al. 2014). When locomotion categorizations are concerned, the cranial view supports for *Arctodus* sp., *Arctotherium bonariense*, and *A. wingei* even the possibility of retaining semiarborescent adaptations in the shape of the elbow joint but not in the size. As the medial epicondyle is particularly

expanded in these species, it is likely that (as for the giant panda) the fossil *Arctodus* and *Arctotherium* retained this character in relation to their higher degree of forelimb dexterity. Mitchell et al. (2016) recently proposed for these genera convergent evolution towards large body size that could have been favored by scavenging adaptations. If this is supported by other paleoecological evidence, then high degree of proximal dexterity could have been advantageous for these species and retained in the Tremarctinae lineage in spite of size evolution.

Paleoecological predictions for Old World Quaternary bears are generally congruent within species. For instance, fossil brown bears are consistently predicted as non-climbing or scansorial in the majority of DFA models except two cases out of 56. Similarly, climbing ability was reduced in *Ursus spelaeus* while the undetermined specimens of *Ursus* from Essex were possibly represented by two distinct morphotypes (one with less ability to climb than the other). Results for *Ursus deningeri* suggest scansoriality to a higher degree of accuracy and confirm previous observations about *U. deningeri* as being more lightly built in the limb apparatus than its descendant *Ursus spelaeus* (Athen 2006). Habitat classification reflects this as *U. deningeri* is categorized as mixed while the majority of cave bears are open (Table 6). In fossil brown bear, habitat predictions generally support adaptations to open environments although mixed and closed categories are predicted in almost half of the cases. This demonstrates a greater variation in the morphology of the elbow joint for Quaternary brown bears as compared to extant specimens. Most of the paleoecological investigations on Quaternary Old World bears concern their dietary adaptations, which appear to be context-dependent but generally congruent towards omnivorous/herbivorous life style (Bocherens et al. 1994, 2006, 2011; Pinto and Andrews 2004; Richards et al. 2008; Pacher and Stuart 2009). Meloro (2011a) predicted for Pleistocene brown bears and cave bears adaptations towards open and closed environments, respectively, based on the brachial index although a closer degree of similarity in limb proportion between cave bears and polar bear was noted. Viranta (1994) also reported for the cave bear a more robust epiphyseal structure and generally thicker bones whose adaptive significance is not entirely clear, as it seems independent of body mass. Considering the broad variation observed in postcranial morphology for fossil brown bears and cave bears (Quiles and Monchot 2004; Athen and Pflretzschner 2005; Santi et al. 2005; Rossi and Santi 2005), it is likely that local adaptations and sexual dimorphism might play a more significant role in interpreting their functional morphology.

The PLS analysis showed a consistent pattern of morphological integration between the cranial and caudal views with variation generally constrained by the expansion of the medial epicondyle in relation to the relative shortening of the trochlea and olecranon region (Fig. 6a). Such a pattern follows two

distinct trajectories in small and large bears and is the result of a trade-off between locomotory adaptation and allometric constraint. Semiarboreal bears with high manual dexterity, like the giant panda, possess a broadly expanded medial epicondyle with a relatively short and wide trochlea and short olecranon region (Fig. 6b); in large cave bears the trochlea expands dorso-ventrally (it become wider and shorter than in the brown bear, so more similar to that of the panda to a certain degree) while the epicondylar region reduces to potentially improve stability at the joint (Fig. 6c). This observation is consistent with our paleoecological interpretation of Quaternary fossil bears and of elbow joint shape variation in Carnivora in general (Andersson and Werdelin 2003).

From a comparative perspective we demonstrate for the first time how isolated elbow joint epiphyses of bears can be investigated to gain insights on Quaternary fossil species. There were no exceptional differences in their shape compared to extant taxa although larger sizes constrained paleoecological interpretations based on this element. Broader taxonomic approaches with the inclusion also of potentially cursorial fossil bears might improve our understanding of bears' ecology and behavior through time.

Acknowledgments This research was supported by the CAPES Foundation, grant: PDSE - 99999.007334/2015-00 awarded to Alessandro Marques de Oliveira. We also want to express our gratitude to museum curators for their support and care during our access to museum collections: P. Jenkins, L. Tomsett, R. Portela-Miguez, D. Hills, A. Salvador, R. Sabin, P. Brewer, and S. Pappa from NHM (London); T. Parker from World Museum (Liverpool); G. Billet, A. Blin, and G. Veron from Museum National d' Histoire Naturelle (Paris). John Wible and two anonymous reviewers kindly provided important insights to improve the quality of this manuscript.

Compliance with Ethical Standards

Conflict of Interest The authors declare that they have no conflict of interest.

Ethical Approval This article does not contain any studies with human participants or animals performed by any of the authors.

Open Access This article is distributed under the terms of the Creative Commons Attribution 4.0 International License (<http://creativecommons.org/licenses/by/4.0/>), which permits unrestricted use, distribution, and reproduction in any medium, provided you give appropriate credit to the original author(s) and the source, provide a link to the Creative Commons license, and indicate if changes were made.

References

- Adams DC, Otárola-Castillo E (2013) geomorph: an R package for the collection and analysis of geometric morphometric shape data. *Meth Ecol Evol* 4:393–399
- Álvarez A, Ercoli MD, Prevosti FJ (2013) Locomotion in some small to medium-sized mammals: a geometric morphometric analysis of the

- penultimate lumbar vertebra, pelvis and hindlimbs. *Zoology* 116: 356–371
- Andersson K (2004) Elbow-joint morphology as a guide to forearm function and foraging behaviour in mammalian carnivores. *Zool J Linn Soc* 142:91–104
- Andersson K, Werdelin L (2003) The evolution of cursorial carnivores in the Tertiary: implications of elbow-joint morphology. *Proc Roy Soc Lond B* 270:S163–S165
- Amaudo ME, Bona P, Soibelzon LH, Schubert BW (2016) Anatomical study of the auditory region of *Arctotherium tarijense* (Ursidae, Tremarctinae), an extinct short-faced bear from the Pleistocene of South America. *J Anat* 229:825–837
- Amaudo ME, Soibelzon LH, Bona P, Schubert B (2014) First description of the auditory region of a Tremarctinae (Ursidae, Mammalia) bear: the case of *Arctotherium angustidens*. *J Mammal Evol* 21:321–330
- Athen K, Pfretzschner HU (2005) Biometrical analysis of postcranial elements of fossil ursids from Einhornhöhle, Germany. *Naturhist Ges Nürnberg eV, Neue Forschungen zum Höhlenbären in Europa* 45: 35–42
- Athen K (2006) Biostatistical investigation of long bones and metapodial bones of *Ursus spelaeus* and *Ursus deningeri*. *Sci Annals, Geol School, AUTH, special* 98: 159–162
- Bassarova M, Janis CM, Archer M (2009) The calcaneum on the heels of marsupial locomotion. *J Mammal Evol* 16:1–23
- Bishop LC (1999) Suid paleoecology and habitat preference at African Pliocene and Pleistocene hominid localities. In: Bromage TG, Schrenk F (eds) *African Biogeography, Climate Change and Human Evolution*. Oxford University Press, Oxford, pp. 216–225
- Bocherens H, Drucker DG, Billiou D, Geneste JJM, Van Der Plicht J (2006) Bears and humans in Chauvet Cave (Vallon-Pont-d'Arc, Ardèche, France): insights from stable isotopes and radiocarbon dating of bone collagen. *J Hum Evol* 50:370–376
- Bocherens H, Fizet M, Mariotti A (1994) Diet, physiology and ecology of fossil mammals as inferred from stable carbon and nitrogen isotope biogeochemistry: implications for Pleistocene bears. *Palaeogeogr Palaeoclimatol Palaeoecol* 107:213–225
- Bocherens H, Stiller M, Hobson KA, Pacher M, Rabeder G, Burns JA, Tütken T, Hofreiter M (2011) Niche partitioning between two sympatric genetically distinct cave bears (*Ursus spelaeus* and *Ursus ingressus*) and brown bear (*Ursus arctos*) from Austria: isotopic evidence from fossil bones. *Quaternary Internat* 245:238–248
- Botton-Divet L, Cornette R, Fabre AC, Herrel A, Houssaye A (2016) Morphological analysis of long bones in semi-aquatic mustelids and their terrestrial relatives. *Integr Comp Biol* 56:1298–1309
- Botton-Divet L, Cornette R, Houssaye A, Fabre AC, Herrel A (2017) Swimming and running: a study of the convergence in long bone morphology among semi-aquatic mustelids (Carnivora: Mustelidae). *Biol J Linn Soc* 121:38–49
- Chom J, Hoffmann RS (1978) *Ailuropoda melanoleuca*. *Mammal Spec* 110:1–6
- Davis DD (1964) The giant panda: a morphological study of evolutionary mechanisms. *Fieldiana Zoology Mem* 3: 1–339
- DeMaster DP, Stirling I (1981) *Ursus maritimus*. *Mamm Species* (145):1
- Elton S (2001) Locomotor and habitat classification of cercopithecoid postcranial material from Sterkfontein Member 4, Bolt's Farm and Swartkrans Members 1 and 2, South Africa. *Palaeontogr Afr* 37: 115–126
- Elton S (2006) Forty years on and still going strong: the use of hominid-cercopithecoid comparisons in palaeoanthropology. *J R Anthropol Inst* 12:19–38
- Elton S, Jansson AU, Meloro C, Louys J, Plummer T, Bishop LC (2016) Exploring morphological generality in the Old World monkey postcranium using an ecomorphological framework. *J Anat* 228: 534–560
- Ercoli MD, Prevosti FJ, Álvarez A (2012) Form and function within a phylogenetic framework: locomotory habits of extant predators and some Miocene Sparassodonta (Metatheria). *Zool J Linn Soc* 165: 224–251
- Fabre AC, Cornette R, Goswami A, Peigné S (2015a) Do constraints associated with the locomotor habitat drive the evolution of forelimb shape? A case study in musteloid carnivores. *J Anat* 226:596–610
- Fabre AC, Cornette R, Peigné S, Goswami A (2013a) Influence of body mass on the shape of forelimb in musteloid carnivores. *Biol J Linn Soc* 110:91–103
- Fabre AC, Cornette R, Slater G, Argot C, Peigné S, Goswami A, Pouydebat E (2013b) Getting a grip on the evolution of grasping in musteloid carnivores: a three-dimensional analysis of forelimb shape. *J Evol Biol* 26:1521–1535
- Fabre AC, Goswami A, Peigné S, Cornette R (2014) Morphological integration in the forelimb of musteloid carnivores. *J Anat* 225:19–30
- Fabre AC, Salesa MJ, Cornette R, Antón M, Morales J, Peigné S (2015b) Quantitative inferences on the locomotor behaviour of extinct species applied to *Simocyon batalleri* (Ailuridae, late Miocene, Spain). *The Science of Nature* 102:1–13
- Figueirido B, Martín-Serra A, Tseng ZJ, Janis CM (2015) Habitat changes and changing predatory habits in North American fossil canids. *Nature Communications* 6:7976.
- Figueirido B, Palmqvist P, Pérez-Claros JA (2009) Ecomorphological correlates of craniodental variation in bears and paleobiological implications for extinct taxa: an approach based on geometric morphometrics. *J Zool* 277:70–80
- Figueirido B, Pérez-Claros JA, Torregrosa V, Martín-Serra A, Palmqvist, P (2010) Demythologizing *Arctodus simus*, the 'short-faced' long-legged and predaceous bear that never was. *J Vertebr Paleontol* 30: 262–275
- Figueirido B, Soibelzon LH (2010) Inferring palaeoecology in extinct tremarctine bears (Carnivora, Ursidae) using geometric morphometrics. *Lethaia* 43:209–222
- Ginsburg L, Morales J (1998) Les Hemicyoninae (Ursidae, Carnivora, Mammalia) et les formes apparentées du Miocène inférieur et moyen d'Europe occidentale. *Ann Paléontol* 84 (1):71–123
- Gittleman JL (1985) Carnivore body size: ecological and taxonomic correlates. *Oecologia* 67:540–554.
- Goldman D, Giri PR, O'Brien SJ (1989) Molecular genetic-distance estimates among the Ursidae as indicated by one- and two-dimensional protein electrophoresis. *Evolution* 43:282–295.
- Grandal-d'Anglade A, López-González F (2005) Sexual dimorphism and ontogenetic variation in the skull of the cave bear (*Ursus spelaeus* Rosenmüller) of the European upper Pleistocene. *Geobios* 38:325–337
- Iwaniuk AN, Pellis SM, Whishaw IQ (2000) The relative importance of body size, phylogeny, locomotion, and diet in the evolution of forelimb dexterity in fissiped carnivores (Carnivora). *Can J Zool* 78: 1110–1125
- Janis CM, Figueirido B (2014) Forelimb anatomy and the discrimination of the predatory behavior of carnivorous mammals: the thylacine as a case study. *J Morphol* 275:1321–1338
- Kappelman J (1988) Morphology and locomotor adaptations of the bovid femur in relation to habitat. *J Morphol* 198:119–130
- Klingenberg CP (2011) MorphoJ: an integrated software package for geometric morphometrics. *Molecular Ecology Resources* 11:353–357
- Klingenberg CP, Marugán-Lobón J (2013) Evolutionary covariation in geometric morphometric data: analyzing integration, modularity, and allometry in a phylogenetic context. *Syst Biol* 62:591–610
- Kovarovik K, Aiello LC, Cardini A, Lockwood CA (2011) Discriminant function analyses in archaeology: are classification rates too good to be true? *J Archaeol Sci* 38:3006–3018
- Krause J, Unger T, Noçon A, Malaspinas AS, Kolokotronis SO, Stiller M, Soibelzon L, Spriggs H, Dear PH, Briggs AW, Bray SC (2008) Mitochondrial genomes reveal an explosive radiation of extinct

- and extant bears near the Miocene-Pliocene boundary. *BMC Evol Biol* 8:220
- Kurtén B (1995) *The Cave Bear Story: Life and Death of a Vanished Animal*. Columbia University Press, New York
- Martín-Serra A, Figueirido B, Palmqvist P (2014) A three-dimensional analysis of morphological evolution and locomotor performance of the carnivoran forelimb. *PLoS One* 9:e85574
- Martín-Serra A, Figueirido B, Palmqvist P (2016) In the pursuit of the predatory behavior of Borophaginae (Mammalia, Carnivora, Canidae): inferences from forelimb morphology. *J Mammal Evol* 23:237–249
- Meachen JA, Dunn RH, Werdelin L (2015) Carnivoran postcranial adaptations and their relationships to climate. *Ecography* 39:553–560
- Meloro C (2011a) Locomotor adaptations in Plio-Pleistocene large carnivores from the Italian Peninsula: palaeoecological implications. *Current Zoology* 57:269–283
- Meloro C (2011b) Feeding habits of Plio-Pleistocene large carnivores as 806 revealed by the mandibular geometry. *J Vertebr Paleontol* 31: 428–446
- Meloro C, Elton S, Louys J, Bishop LC, Ditchfield P (2013) Cats in the forest: predicting habitat adaptations from humerus morphometry in extant and fossil Felidae (Carnivora). *Paleobiology* 39:323–344
- Meloro C, Hudson A, Rook L (2015) Feeding habits of extant and fossil canids as determined by their skull geometry. *J Zool* 295:178–188
- Meloro C, Louys J (2015) Ecomorphology of radii in Canidae: application to fragmentary fossils from Plio-Pleistocene hominin assemblages. *Acta Palaeontol Pol* 60:795–806
- Milne N, Toledo N, Vizcaino SF (2012) Allometric and group differences in the xenarthran femur. *J Mammal Evol* 19: 199–208.
- Mitchell KJ, Bray SC, Bover P, Soibelzon L, Schubert BW, Prevosti F, Prieto A, Martin F, Austin JJ, Cooper A (2016) Ancient mitochondrial DNA reveals convergent evolution of giant short-faced bears (Tremarctinae) in North and South America. *Biol Lett* 12:20160062
- Ortolani A, Caro TM (1996) The adaptive significance of color patterns in carnivores: phylogenetic tests of classic hypotheses. In Gittleman JL (ed) *Carnivore Behavior, Ecology, and Evolution*, Vol. 2. Comstock, Ithaca, pp 132–188
- Pacher M, Stuart AJ (2009) Extinction chronology and palaeobiology of the cave bear (*Ursus spelaeus*). *Boreas* 38:189–206
- Pinto AC, Andrews PJ (2004) Scavenging behaviour patterns in cave bears *Ursus spelaeus*. *Revue de Paléobiologie* 23:84
- Plummer TW, Bishop LC, Hertel F (2008) Habitat preference of extant African bovids based on astragalus morphology: operationalizing ecomorphology for palaeoenvironmental reconstruction. *J Archaeol Sci* 35:3016–3027
- Prevosti FJ, Martin FM (2013) Paleocology of the mammalian predator guild of southern Patagonia during the latest Pleistocene: ecomorphology, stable isotopes, and taphonomy. *Quaternary Internatl* 305:74–84
- Prevosti FJ, Vizcaino SF (2006) Paleocology of the large carnivore guild from the late Pleistocene of Argentina. *Acta Palaeontol Pol* 51:407–422
- Preuß A, Gansloßer U, Purschke G, Magiera U (2009) Bear-hybrids: behaviour and phenotype. *Der Zoologische Garten* 78: 204–220
- Quiles J, Monchot H (2004) Sex-ratio et analyse des mélanges d'*Ursus spelaeus* (Carnivora, Ursidae) du gisement pléistocène supérieur de Fate (Ligurie, Italie). Implications paléobiologiques. *Ann Paléontol* 90 :115–133.
- Richards MP, Pacher M, Stiller M, Quilès J, Hofreiter M, Constantin S, Zilhão J, Trinkaus E (2008) Isotopic evidence for omnivory among European cave bears: late Pleistocene *Ursus spelaeus* from the Peștera cu Oase, Romania. *Proc Natl Acad Sci USA* 105:600–604
- Rohlf FJ (2015) The tps series of software. *Hystrix, the Italian Journal of Mammalogy* 26:9–12
- Rohlf FJ, Corti M (2000) Use of two-block partial least-squares to study covariation in shape. *Syst Biol* 49:740–753
- Rohlf FJ, Slice D (1990) Extensions of the Procrustes method for the optimal superimposition of landmarks. *Syst Biol* 39:40–59
- Rossi M, Santi G (2005) First morphometric data from the metapodial bones of *Ursus* from Cerè Cave (Venetia Region, North Italy). *Cranium* 22:13–25
- Sacco T, Van Valkenburgh B (2004) Ecomorphological indicators of feeding behaviour in the bears (Carnivora: Ursidae). *J Zool* 263:41–54
- Samuels JX, Meachen JA, Sakai SA (2013) Postcranial morphology and the locomotor habits of living and extinct carnivorans. *J Morphol* 274:121–146
- Samuels JX, Van Valkenburgh B (2008) Skeletal indicators of locomotor adaptations in living and extinct rodents. *J Morphol* 269:1387–1411
- Santi G, Rossi M, Fonte A (2005) Morphometry of the limb bones of the *Ursus spelaeus* Rosemuller, 1794 from Valstrona (Piedmont-Northern Italy). *Revue de Paléobiologie*, 24: 597–616
- Schutz H, Guralnik RP (2007) Postcranial element shape and function: assessing locomotor mode in extant and extinct mustelid carnivorans. *Zool J Linn Soc* 150:895–914
- Soibelzon LH, Grinspan GA, Bocherens H, Acosta WG, Jones W, Blanco ER, Prevosti F (2014) South American giant short-faced bear (*Arctotherium angustidens*) diet: evidence from pathology, morphology, stable isotopes, and biomechanics. *J Paleontol* 88:1240–1250
- Soibelzon LH, Pomi LH, Tonni EP, Rodriguez S, Dondas A (2009) First report of a South American short-faced bears' den (*Arctotherium angustidens*): palaeobiological and palaeoecological implications. *Alcheringa* 33:211–222
- Sorkin B (2006) Ecomorphology of the giant bear-dogs *Amphicyon* and *Ischyrocyon*. *Historical Biology* 18:375–388
- Stefen C (2001) Enamel structure of arctoid carnivora: Amphicyonidae, ursidae, procyonidae, and mustelidae. *Journal of Mammalogy* 82 (2):450–462
- Tarquini J, Toledo N, Morgan CC, Soibelzon LH (2017) The forelimb of *Cyonasua* sp. (Procyonidae, Carnivora): ecomorphological interpretation in the context of carnivorans. *Earth Environ Sci Trans R Soc Edinb* 106:325–335
- van Heteren AH, MacLarnon A, Soligo C, Rae TC (2014) Functional morphology of the cave bear (*Ursus spelaeus*) cranium: a three-dimensional geometric morphometric analysis. *Quaternary Internatl* 339:209–216.
- van Heteren AH, MacLarnon A, Soligo C, Rae TC (2016) Functional morphology of the cave bear (*Ursus spelaeus*) mandible: a 3D geometric morphometric analysis. *Org Divers Evol* 16:299–314
- Van Valkenburgh B (1987) Skeletal indicators of locomotor behavior in living and extinct carnivores. *J Vertebr Paleontol* 7:162–182
- Viranta, S. (1994). Limb bone proportions and body mass of the cave bear (*Ursus spelaeus*). *Hist Biol* 7(3):239–250
- Waits LP, Sullivan J, O'Brien SJ, Ward RH (1999) Rapid radiation events in the family Ursidae indicated by likelihood phylogenetic estimation from multiple fragments of mtDNA. *Mol Phylogen Evol* 13:82–92
- Walmsley A, Elton S, Louys J, Bishop LC, Meloro C (2012) Humeral epiphyseal shape in the Felidae: the influence of phylogeny, allometry, and locomotion. *J Morphol* 273:1424–1438